Solvent and rotational relaxation of coumarin-153 and coumarin-480 in ionic liquid (1-butyl-3-methylimidazolium tetrafluoroborate) modified sodium 1,4-bis(2-ethylhexyl) sulfosuccin...

ARTICLE *in* SPECTROCHIMICA ACTA PART A MOLECULAR AND BIOMOLECULAR SPECTROSCOPY · NOVEMBER 2012

Impact Factor: 2.35 · DOI: 10.1016/j.saa.2012.10.036 · Source: PubMed

Spectrochimica Acta Part A: Molecular and Biomolecular Spectroscopy 102 (2013) 371–378

Contents lists available at SciVerse ScienceDirect

Spectrochimica Acta Part A: Molecular and Biomolecular Spectroscopy

journal homepage: www.elsevier.com/locate/saa

Solvent and rotational relaxation of coumarin-153 and coumarin-480 in ionic liquid (1-butyl-3-methylimidazolium tetrafluoroborate) modified sodium 1,4-bis(2-ethylhexyl) sulfosuccinate (NaAOT) micelle

Vishal Govind Rao, Chiranjib Banerjee, Sarthak Mandal, Surajit Ghosh, Nilmoni Sarkar *

Department of Chemistry, Indian Institute of Technology, Kharagpur 721 302, WB, India

HIGHLIGHTS

- We have shown how IL addition to aqueous surfactant solution can affect the solvation dynamics.
- We have chosen two probes of different polarities to probe the dynamics at two different sites.
- We have shown the probe dependent solvation dynamics owing to difference in their location.

GRAPHICAL ABSTRACT

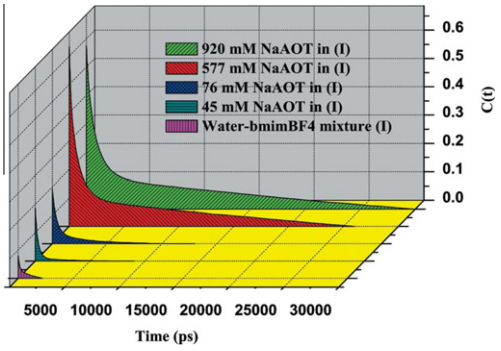

ARTICLE INFO

Article history:
Received 16 July 2012
Received in revised form 17 October 2012
Accepted 22 October 2012
Available online 1 November 2012

Keywords:
Solvent relaxation
Rotational relaxation
Hydrophobicity
Amphiphile
Ionic liquid

ABSTRACT

Understanding ion transport dynamics, structure of surfactant aggregates in ionic liquids or ionic liquid/water solutions are quite interesting and potentially important due to widespread applications of surfactant-based systems. In this manuscript we have investigated the effect of 1-butyl-3-methylimidazolium tetrafluoroborate ($bmimBF_4$) addition on solvent and rotational relaxation of coumarin-153 (C-153) and coumarin-480 (C-480) in aqueous solution of sodium 1,4-bis(2-ethylhexyl) sulfosuccinate (NaAOT) using steady state and picosecond time resolved fluorescence spectroscopy. The strong adsorption of the $bmim^+$ at the interface and the role of the ionic liquid particularly the cation $bmim^+$ in the modification of the interfacial geometry were probed by the analysis of decay parameters and the rotational relaxation parameters. Since the addition of the NaAOT in water–$bmimBF_4$ mixture above critical micellar concentration (48 mM, obtained from observing pyrene fluorescence) causes strong adsorption of the ionic liquid particularly the cation $bmim^+$, the average solvation time, particularly the slow component increases significantly. More importantly we have found the probe dependent solvation dynamics due to the different location of the probe molecules, C-153 and C-480. C-153 being hydrophobic in nature resides in the stern layer and the adsorption of the $bmim^+$ at the interface modifies stern layer more effectively. So we have observed more pronounced change in solvation dynamics in case of C-153 compared to that in case of C-480. The fluorescence anisotropy decays of the probe molecules were found to be biexponential in nature. The anisotropy decay was interpreted by using a model which consists of the wobbling (rotational) and translational diffusion of the dye coupled with the rotational motion of the micelle as a whole.

* Corresponding author. Tel.: +91 3222 283332; fax: +91 3222 255303.
E-mail address: nilmoni@chem.iitkgp.ernet.in (N. Sarkar).

1386-1425/$ - see front matter © 2012 Elsevier B.V. All rights reserved.
http://dx.doi.org/10.1016/j.saa.2012.10.036

Introduction

From the last decade room temperature ionic liquids have become the focal point of green chemistry [1] due to their unique properties, such as, low vapor pressure, high thermal stability, wide liquidous temperature range, wide electro chemical window, and their applicability as "designer solvents" because their physical properties can be varied predictably by incorporation of appropriate functional groups [2–5]. Due to these properties, the RTILs have been successfully used in many applications, including replacing traditional organic solvent in organic and inorganic synthesis, [6] solvent extraction with crown ether, [7] liquid–liquid extractions with supercritical fluid CO_2, [8,9] electrochemical reactions, [10] and as a medium for enzyme reactions [11]. Not only this, self assembly of surfactants in contact with ionic liquids, the former thereby forming micelles, [12–14] microemulsions, [15–17] liquid crystals, [18] gels, [19] and vesicles, [20] has been extensively explored.

Apart from the use of ionic liquid as a solvent in the self assembly of surfactant molecules, it can be used as additive. Modification of physicochemical properties of aqueous surfactant solutions in favorable fashion by addition of environmentally benign room-temperature ionic liquids (ILs) has enormous future potential. When ionic liquids are added as additive, the electrolytic/surfactant/cosolvent nature of ionic liquid may produce significant change in the morphology typically manifested by the surfactant in a suitable solvent. Pandey et al. [21–25] have shown the change in the behavior of aqueous surfactant solutions with the addition of RTILs. Considering ILs as salt solutions may offer an explanation of their effect on micellar and biological systems. The lowering of CMC of a micellar solution on the addition of a salt has been ascribed to the decreased repulsion between the head groups of the surfactant molecules as a direct consequence of the salt addition (salt effect, the so-called Hofmeister effect [26]). This lowering of repulsion lends stability to the micelles which is consequently manifested as a lowering of the CMC value of the surfactant solution. However, in explaining the monotonic as well as nonmonotonic effect on the CMC of surfactant solutions that is observed on addition of ILs to the same, one cannot apply a similar line of reasoning. In case of sodium dodecyl sulfate (SDS), both increment and decrement of CMC has been observed on addition of $bmimBF_4$, the former and the latter being observed on addition of low and high concentrations of $bmimBF_4$, respectively [21]. Smirnova et al. [27] have shown that the CMC of sodium dodecyl sulfate (SDS), decreases monotonically with the addition of long chained ILs capable to form micelles in their individual aqueous solutions. In many cases, addition of the IL does not significantly alter the CMC values, rather the structure of the micelles are modified to a great extent [28]. Zheng et al. showed that addition of the IL 1-butyl-3-methylimidazolium bromide ([bmim][Br]) affects aggregation of the triblock copolymer Pluornic P104, and at a high concentration of the RTIL (>1 M) very large aggregates with a diameter of ~500 nm are formed [29]. Recently, Dey et al. showed that the addition of IL (RTIL, [pmim][Br]) to a 5 wt.% triblock copolymer (P123) micelle leads to the formation of giant P123-RTIL clusters of 40 nm in 0.9 M and 3500 nm in 3 M RTIL [30]. Sizes of both of these clusters are much larger than the P123 micelle (18 nm).

Rogers and Winsor have reported that sodium 1,4-bis(2-ethylhexyl) sulfosuccinate (NaAOT) forms extended lamellar shaped micelles at low concentration which changes to a bicontinuous cubic phase and finally to a reverse hexagonal phase with increase in concentration of NaAOT [31]. Recently Murgia et al. [32] have noted the effect of addition of 1-butyl-3-methylimidazolium tetrafluoborate ($bmimiBF_4$) on the morphology of a well known surfactant/water system, i.e. the NaAOT/water (W) system. They have studied the phase behavior of the NaAOT/W/$bmimBF_4$ and reported the formation of spherical micelle at different compositions. They highlighted the role of the large $bmim^+$ cation, particularly on its partition between bulk and the NaAOT interface. Understanding the dynamics of $bmimBF_4$ particularly the $bmim^+$ cation can further provide useful information regarding this system.

The study of solvation dynamics and the manner in which it affects chemical reactions such electron transfer charge transfer processes continues till date because of its importance [33–48]. For a complete understanding of the chemical reactivity of a species, knowledge about the influence of the surrounding solvent on the electronic transition of a molecule of that species is absolutely essential. In order to obtain molecular level information about the response of solvent molecules to a probe, the technique of studying the solvation dynamics of a newly created ion or a dipole in polar liquids is currently in use [34–36]. The response of the solvent molecules to the probe molecule has contributions from both orientational and translational motions. Solvation dynamics, as a probing technique allows one to distinguish, at least partly, between local and bulk contributions. It can provide detailed insight into the microenvironments of the probe locations in microheterogeneous media. However, it suffers from limitation that the changes occurring at long distances from the probe cannot be monitored. There have been extensive studies on solvation dynamics in different heterogeneous media and restricted environments such as micelles, reverse micelles, lipids, proteins, and DNA [34–49]. Water seems to be by far the 'fastest' solvent studied so far: simulations predict that well over half of the solvation response for atomic solutes is inertial, happening on a timescale of about 20 fs [50,51] and the remaining solvation occurs in the range of $\leqslant$50 ps, this component arises due to the diffusive motion of hydrogen bonded water molecule clusters. There are many literature reports which deal with the solvation in aqueous media [52]. The dynamic exchange model has often been used to explain bimodal solvent relaxation [52]. Recent computer simulations [53] also support this fact. These studies [54,55] showed that the hydrogen bonding between water molecules and surfactant is much stronger than the hydrogen bond between the two water molecules. So these two types of water molecules are responsible for the slow and fast component of the solvation dynamics. It should be noted that solvation dynamics in RTILs are vastly different from that in the isopolar conventional solvents such as methanol, and acetonitrile [56,57]. Recent ultrafast studies suggest that the difference is less striking than originally thought [58,59]. Chapman and Maroncelli [60] showed that ionic solvation is slower compared to the pure solvent and dependent on the viscosity of the medium. Bart et al. [61] showed that ionic solvation is slow and biphasic in nature. Samanta et al. [62,63] ascribed that the fast component is due to the anions and the slow component is attributed to large-scale rearrangement of the ions around the photoexcited system. Petrich and co-workers observed that the polarizability of the cation is responsible for the fast component [64,65]. Song observed the similar phenomenon regarding fast components using Debye–Huckel dielectric continuum model [66]. Halder et al. [67] suggest that translational motion of ions may not be the predominant factor in the short time solvation of ionic fluids. While Shim et al. have shown that the short component is due to the translational motion of the anion, [68] Kobrak and Znamenskiy, on the other hand, have demonstrated that collective cation–anion motion is responsible for the fast component [69]. Simulation studies also suggest that solvation dynamics in RTIL involves collective motion of cations and the anions [70]. According to present theory of Kashyap and Biswas [71] fast component of the solvation re-

sponse function originates from the rapid orientational relaxation involving the dipolar species, whereas the relaxation of the ion dynamic structure factor via ion translation produces the observed slow nonexponential component.

In our study, we have applied steady state and picosecond time resolved fluorescence spectroscopy to investigate the effect of 1-butyl-3-methylimidazolium tetrafluoroborate ($bmimBF_4$) addition on solvent and rotational relaxation of coumarin-153 (C-153) and coumarin-480 in aqueous solution of sodium 1,4-bis(2-ethylhexyl) sulfosuccinate (NaAOT).

Experimental section

The coumarin 153 (C-153) and coumarin 480 (C-480) (laser grade, Exciton) was used as received. The RTIL, 1-butyl-3-methylimidazolium tetrafluoroborate ($bmimBF_4$) was obtained from Kanto chemicals (98% purity) and purified further using the literature procedure [62]. The RTIL was dried in vacuum for 24 h at 70–80 °C before use. NaAOT (sodium 1,4-bis(2-ethylhexyl) sulfosuccinate, Sigma–Aldrich) was dried in vacuum for 30 h before use. Pyrene was purchased from Sigma–Aldrich and used as received. Milli-Q water was used for sample preparation. The structure of C-153, $bmimBF_4$ and NaAOT is shown in Scheme S1 of Supporting Information. The final concentration of the probe molecule (C-153), in all the measurements was kept $\sim 8 \times 10^{-6}$ M. The stock solution of pyrene was prepared in ethanol and the final concentration of pyrene was kept at 2×10^{-6} M in all the measurements. The names for different sample compositions are given in Table 1.

The absorption and fluorescence spectra were collected using a Shimadzu (model no. UV-2450) spectrophotometer and a Hitachi (model no. F-7000) spectrofluorimeter respectively. For steady-state experiments, all the samples were excited at 410 nm. The detailed time-resolved fluorescence setup is described in our earlier publication [72]. The temperature was kept constant (298 K) by circulating water through the cell holder using a Neslab Thermostat (RTE7). For dynamic light scattering (DLS) measurements, we used a Malvern Nano ZS instrument employing a 4 mW He–Ne laser operating at a wavelength of 633 nm and an avalanche photodiode (APD) detector. All measurements reported were performed at 298 K. For viscosity measurements at 298 K, we used a Brookfield DV-II + Pro (viscometer).

The time resolved fluorescence anisotropy $r(t)$ is calculated using the following equation:

$$r(t) = \frac{I_{\parallel}(t) - GI_{\perp}(t)}{I_{\parallel}(t) + 2GI_{\perp}(t)} \quad (1)$$

where G is the correction factor for detector sensitivity to the polarization direction of emission, $I_{\parallel}(t)$ and $I_{\perp}(t)$ are fluorescence decays polarized parallel and perpendicular to the polarization of the excitation light, respectively.

The time-resolved emission spectra (TRES) were constructed by the following procedure of Fleming and Maroncelli [33,73]. The peak frequency evaluated from log-normal fitting of TRES was then used to construct the decay of the solvent correlation function $C(t)$, which is defined as:

$$C(t) = \frac{\nu(t) - \nu(\infty)}{\nu(0) - \nu(\infty)} \quad (2)$$

$\nu(0)$ is the frequency at "zero-time", as calculated by the full method of Maroncelli, [73] $\nu(\text{"}\infty\text{"})$ is the frequency at "infinite time", which may be taken as the maximum of the steady-state fluorescence spectrum if solvation is more rapid than the population decay of the probe, $\nu(t)$ is determined by taking the maxima from the log-normal fits as the emission maximum. In most of the cases, however, the spectra are broad, so there is some uncertainty in the exact position of the emission maxima. Therefore, following Petrich et al. [64,65,74] we have considered the range of the raw data points in the neighborhood of the maximum to estimate an error for the maximum obtained from the log-normal fit. Depending on the width of the spectrum (i.e. zero-time, steady state, or TRES), we have determined the typical uncertainties as follows: zero time - $\approx$ steady-state ($110\ cm^{-1}$) < time resolved ($200\ cm^{-1}$) emission. We use these uncertainties to compute error bars for $C(t)$. Finally, in generating $C(t)$, the first point was obtained from the zero time spectrum. The second point was taken at the maximum of the instrument response function, which, having a full width at half-maximum of $\leqslant$100 ps, was taken to be 100 ps. Finally the time dependence of the calculated $C(t)$ values was fitted by a biexponential function for **I**, **II** and **VI**, and by a triexponential function for **III**, I**V**, and **V**. The biexponential and triexponential functions are as follows

$$c(t) = a_1 e^{-t/\tau_1} + a_2 e^{-t/\tau_2} \quad (3)$$

$$c(t) = a_1 e^{-t/\tau_1} + a_2 e^{-t/\tau_2} + a_3 e^{-t/\tau_3} \quad (4)$$

where τ_1, τ_2, τ_3, are the solvent relaxation time constants ($\geqslant$100 ps, below this we are missing owing to our instrumental resolution) and a_1, a_2 and a_3 are normalized pre-exponential factors. The average solvation time (τ_{av}) is calculated as:

$$\tau_{av} = a_1\tau_1 + a_2\tau_2 + a_3\tau_3 \quad (5)$$

Table 1
Sample name for different sample compositions.

Sample composition	Sample name
Water–$bmimBF_4$ mixture (in 1:1 weight ratio)	**I**
45 mM NaAOT in water–$bmimBF_4$ mixture (in 1:1 weight ratio)	**II**
76 mM NaAOT in water–$bmimBF_4$ mixture (in 1:1 weight ratio)	**III**
577 mM NaAOT in water–$bmimBF_4$ mixture (in 1:1 weight ratio)	**IV**
920 mM NaAOT in water–$bmimBF_4$ mixture (in 1:1 weight ratio)	**V**
4 mM NaAOT in water	**VI**

Results and discussion

Determination of critical micelle concentration (CMC) from pyrene fluorescence

The unique response of pyrene fluorescence to the solvent polarity has been utilized to determine the CMC of NaAOT in Water–$bmimBF_4$ mixture (in 1:1 weight ratio). The ratio of fluorescence intensities of the first and third vibronic bands, I_I/I_{III} decreases with decreasing solvent dipolarity. With the micelle formation the nonpolar pyrene molecule partitions into the "hydrophobic" micellar phase, resulting in an abrupt decrease in I_I/I_{III}. This abrupt decrease in I_I/I_{III} forms the basis of CMC determination for micelle forming surfactant solutions. Fig. S1 of Supporting Information represents pyrene I_I/I_{III} versus [NaAOT]. The data were fitted with sigmoidal expression. The critical micelle concentration (CMC) of NaAOT in a mixture of water and $bmimBF_4$ (in 1:1 weight ratio) was found to be 48 mM, which is almost 17 times higher than the CMC of NaAOT in water (2.8 mM). This higher CMC in water and $bmimBF_4$ mixture (in 1:1 weight ratio) clearly indicates the cosolvent nature of $bmimBF_4$. The low solvophobicity between the IL and hydrophobic tail of surfactant molecule leads to a high CMC, which is well supported by earlier reports [21,75].

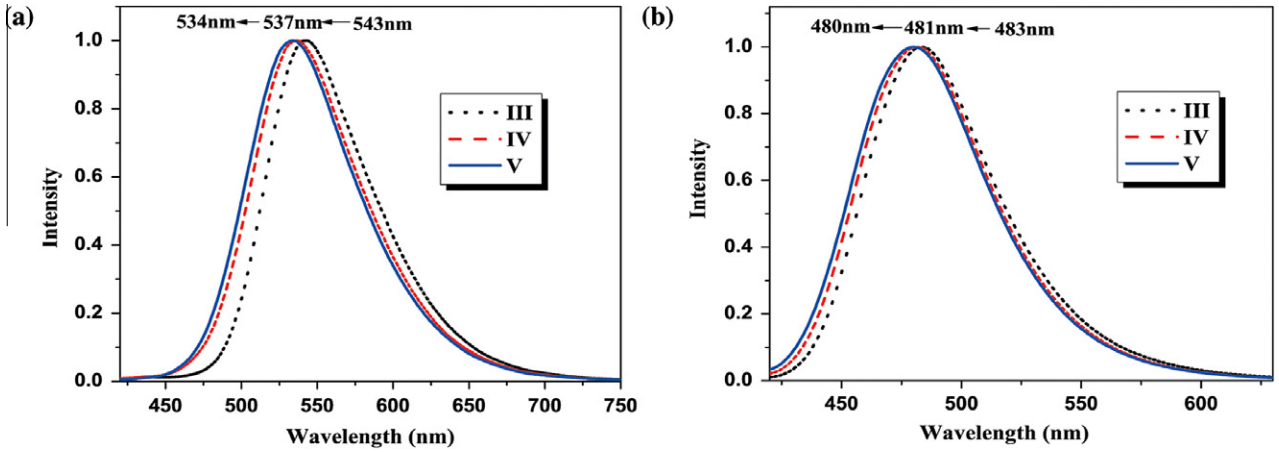

Fig. 1. Emission spectra of: (a) C-153 and (b) C-480 in different systems.

Absorption and steady-state fluorescence measurements

The absorption and emission spectra of C-153 and C-480 in all the measurements were recorded at 298 K. The absorption and emission maxima of C-153 and C-480 in different systems are given in Table S1 of the Supporting Information. The emission maximum of C-153 is blue shifted by 9 nm with the addition of 4 mM NaAOT in water, which clearly indicates that the probe molecule resides in nonpolar environment. Both the absorption and emission peaks of C-153 and C-480 in **I**, **II**, **III**, **IV**, and **V** are blue shifted compared to that in water and are red shifted compared to that in neat ionic liquid. With the addition of 76 mM of NaAOT to **I** (just above CMC) the emission maxima changes from 547 to 543 nm and 485 to 483 nm in case of C-153 and C-480 respectively. So in case of C-153 we have observed a change of 4 nm whereas only 2 nm change is observed in case of C-480. From this comparison we can say that the both the dye molecule resides near the surface, this observation is consistent with the observation by the other group: practically all organic molecules are solubilized near the surface even for small organic molecule such as benzene [40]. The large change in emission maximum in case of C-153 compared to that of C-480 can be explained by the fact that C-153 is more hydrophobic compared to C-480, hence after micelle formation it prefers more hydrophobic region and goes inside the micelle (in stern layer), whereas C-480 resides at the extreme outermost surface. The gradual blue shift observed in the emission maxima of C-153 and C-480 with increasing concentration of NaAOT (Fig. 1) can be explained by the fact that the ionic liquid particularly the cation ($bmim^+$) get attached to the AOT^-, [32] hence the polarity sensed by the probe molecules changes at higher concentrations of NaAOT. The polarity sensed by probe molecule becomes almost equal to that of neat ionic liquid in **V**. In all the cases the emission spectra (emission maxima) is independent of the excitation wavelength, so we can say that all the dye molecule are in same microscopic environment.

Determination of average aggregate size from dynamic light scattering method

We have used dynamic light scattering (DLS) method to obtain the average size of the aggregates of the NaAOT micelle in water–$bmimBF_4$ mixture. Table S2 of Supporting Information summarizes the number average hydrodynamic diameters in nanometers and the polydispersity index values for each sample. The number average hydrodynamic diameters increase with the loading of NaAOT to water–$bmimBF_4$ mixture (Fig. 2).

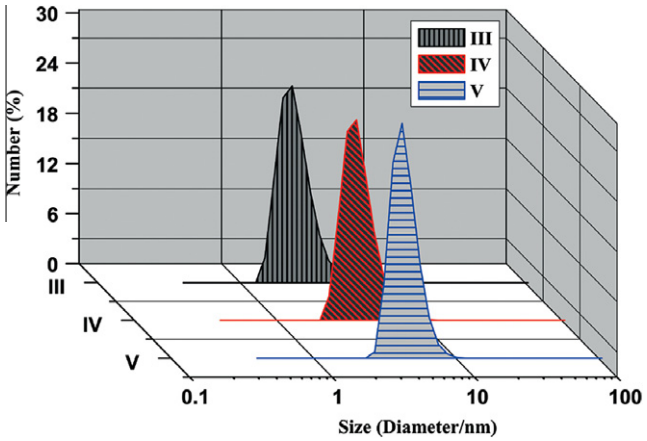

Fig. 2. Number average size distribution (measured by dynamic light scattering) for different systems.

Time resolved studies

Time resolved fluorescence anisotropy

The time constant of fluorescence anisotropy decay of C-153 and C-480 in bulk water was found to be 0.10 ns and 0.12 ns respectively. The time constant of fluorescence anisotropy decay of C-153 and C-480 in the highly viscous RTIL $bmimBF_4$ are 3.19 ns and 3.52 ns respectively, this can be accounted by considering the viscosity of the RTIL. The fluorescence anisotropy decays of C-153 and C-480 are shown in Fig. 3. In our case the anisotropy decay is best fitted by biexponential function which consists of both slow and fast components. The biexponential nature of rotational relaxation decay in micelles is neither due to two different locations of probe molecule in the micelle nor due to the anisotropic rotation of the probe. The observed biexponential nature of rotational relaxation is due to the different types of motion of probe molecules in the micelle. The anisotropy results are summarized in Table 2. The rotational relaxation time of C-153 and C-480 increases with the loading of NaAOT to water–$bmimBF_4$ mixture, which indicates that the rotation of C-153 and C-480 get hindered with the loading of NaAOT. We have calculated several rotational parameters using wobbling in a cone model [76–78]. This model describes the fact that observed slow rotational relaxation is a convolution of the relaxation time corresponding to the overall rotation of the micelles (τ_M) and lateral diffusion of the monomers in

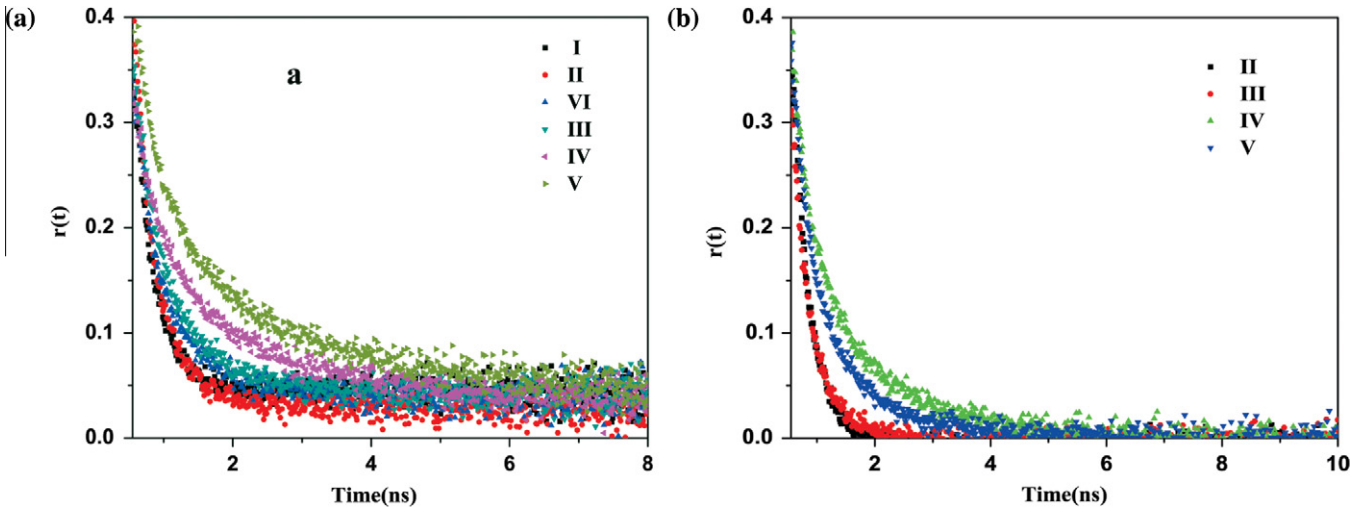

Fig. 3. Time resolved fluorescence anisotropy decay of: (a) C-153 and (b) C-480 in different systems.

Table 2
Anisotropy decay parameters of C-153 and C-480 in different systems.

System	a_{1r}	τ_{slow} (ns)	a_{2r}	τ_{fast} (ns)	$<\tau_{rot}>$[a] (ns)	Viscosity (cp)[a]
C-153 in water			1.00	0.10	0.10	0.9
C-153 in **I**	0.02	0.71	0.98	0.30	0.29	1.5
C-153 in **II**	0.48	0.48	0.52	0.19	0.33	2.3
C-153 in **III**	0.20	1.14	0.80	0.39	0.54	4.0
C-153 in **IV**	0.38	1.89	0.62	0.41	0.97	10.7
C-153 in **V**	0.46	2.07	0.54	0.37	1.15	28.2
C-153 in **VI**	0.45	0.78	0.55	0.22	0.47	1.0
C-153 in $bmimBF_4$[b]	0.85	3.65	0.15	0.61	3.19	100.0
C-480 in water			1.00	0.12	0.12	0.9
C-480 in **I**	0.03	0.70	0.97	0.30	0.31	1.5
C-480 in **II**	0.42	0.49	0.58	0.20	0.32	2.3
C-480 in **III**	0.29	0.75	0.71	0.25	0.40	4.0
C-480 in **IV**	0.36	1.29	0.64	0.34	0.68	10.7
C-480 in **V**	0.44	1.81	0.56	0.41	1.03	28.2
C-480 in **VI**	0.32	0.74	0.68	0.13	0.32	1.0
C-480 in $bmimBF_4$[c]	1.0	3.52			3.52	100.0

[a] Error in experimental data of ±5%.
[b] These data's in neat ionic liquid ($bmimBF_4$) is taken from Ref. [80].
[c] These data's in neat ionic liquid ($bmimBF_4$) is taken from Ref. [81].

the micelle (τ_D). This also describes the internal motion of the probe (τ_R) in terms of cone angle (θ_0) and wobbling diffusion coefficient (D_W). These parameters are obtained by the following equations:

$$1/\tau_{slow} = 1/\tau_D + 1/\tau_M \quad (6)$$

$$1/\tau_{fast} = 1/\tau_R + 1/\tau_D + 1/\tau_M \quad (7)$$

where τ_{slow} and τ_{fast} are the observed fast and slow components. For obtaining all the parameters discussed above we need to know the value of τ_M. For a spherical particle τ_M can be calculated by Stokes–Einstein relation:

$$\tau_M = \frac{\eta 4\pi r_h^3}{3kT} \quad (8)$$

where η is the viscosity of the bulk medium, r_h is hydrodynamic radius of the micelle, and k and T are the Boltzmann constant and absolute temperature respectively. The translational diffusion coefficient of the probe (D_t) is related to τ_D by the following equation:

$$D_t = \frac{r_h^2}{6\tau_D} \quad (9)$$

Table 3
Analytical rotational parameters of C-153 and C-480 in different systems.

Systems	τ_M (ns)	τ_R (ns)	τ_D (ns)	$D_W \times 10^{-8}$ (s^{-1})	$D_t \times 10^{10}$ (m^2s^{-1})	θ_0 (°)	S
C-153 in **III**	7.95	0.59	1.33	4.54	1.96	55.1	0.45
C-153 in **IV**	74.71	0.52	1.94	3.29	3.10	43.9	0.62
C-153 in **V**	326.99	0.45	2.08	3.14	4.05	39.9	0.68
C-480 in **III**	7.95	0.37	0.83	5.77	3.14	49.2	0.54
C-480 in **IV**	74.71	0.46	1.32	3.95	4.56	45.2	0.60
C-480 in **V**	326.99	0.53	1.82	2.90	4.63	41.2	0.66

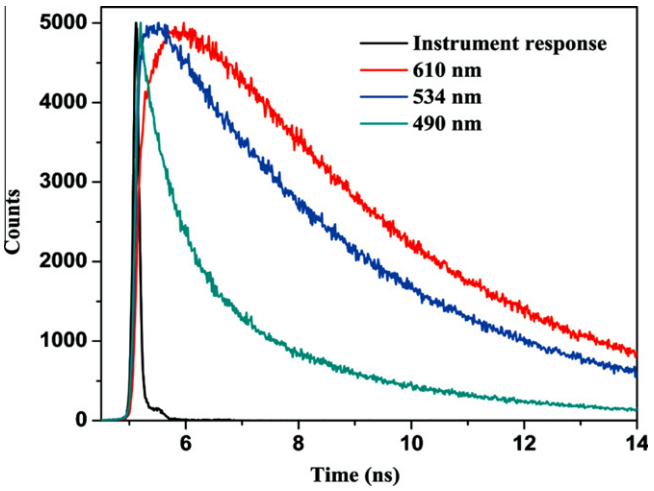

Fig. 4. Fluorescence decay of C-153 in V at different wavelength.

We have calculated the order parameters (S) from the following equation to know the exact location of the probe:

$$a_{1r} = S^2 \quad (10)$$

where a_{1r} is the pre exponential factor for the slow component of the rotational relaxation, S^2 is the square of order parameter (which is a measure of the equilibrium orientational distribution of the dye [78]). We have calculated the cone angle and θ_0 and wobbling diffusion constant D_W as follows:

$$\theta_0 = \cos^{-1}\left[\frac{1}{2}((1+8S)^{1/2} - 1)\right] \quad (11)$$

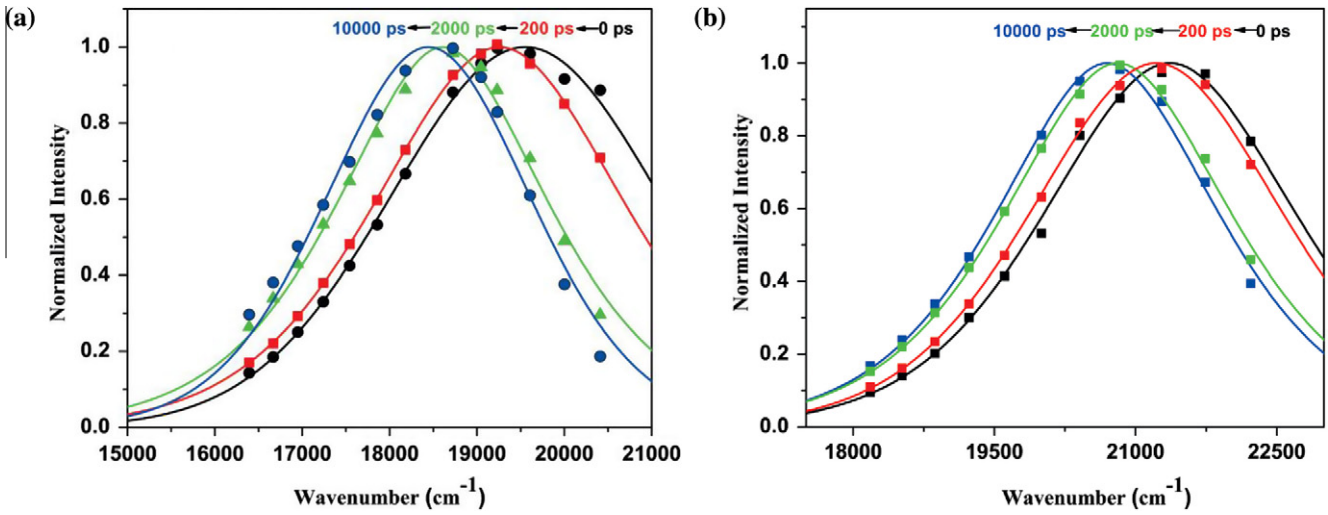

Fig. 5. Time resolved emission spectra of: (a) C-153 and (b) C-480 in V.

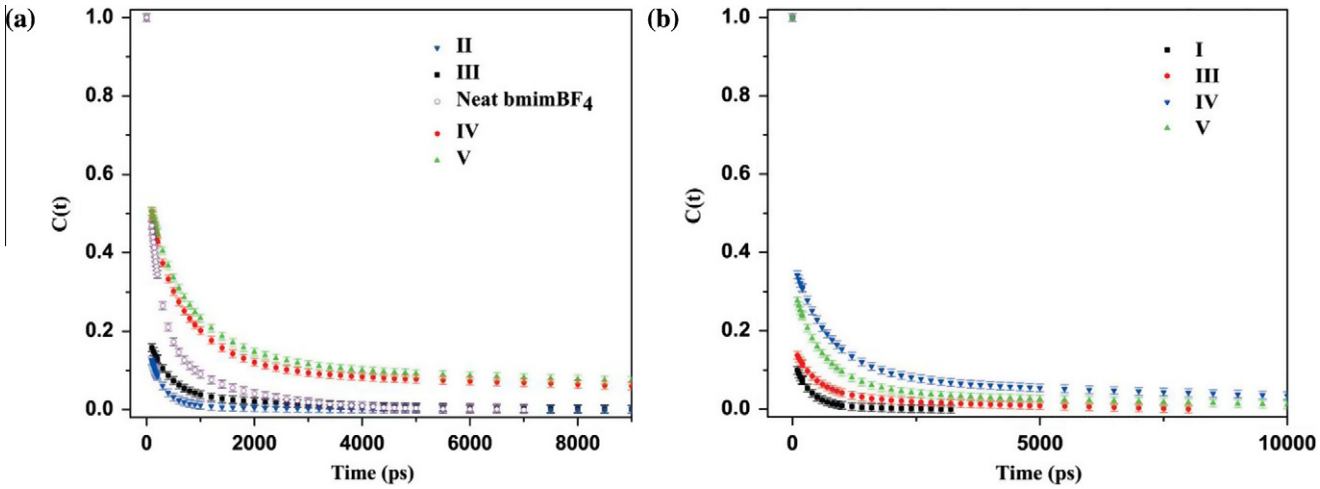

Fig. 6. Decay of solvent correlation function $C(t)$ of: (a) C-153 and (b) C-480 in different systems.

$$D_w = \frac{7\theta^2}{24\tau_R} \tag{12}$$

where θ is the cone angle in radians, and the magnitude of S is a measure of spatial restriction and has value from zero (unrestricted motion) to 1 (completely restricted motion).

The values of τ_M, τ_R, τ_D, D_W, D_t, θ_0, and S were calculated and are given in Table 3. The obtained parameters clearly indicate that the value of θ_0 decreases and the value of S increases for both the probe molecules with increase in surfactant concentration. The growing steric hindrance is responsible for the decrease of θ_0 and increase of S with increase in surfactant concentration. D_W and θ_0 are the quantitative parameters for the wobbling in a cone model. Magnitude of D_W is a measure of freeness of the wobbling motion. The higher value of D_W indicates that wobbling motion is free. The slow wobbling at higher surfactant concentration (as indicated by Table 3) can be attributed to the increase in the viscosity. From Table 3 it is clear that D_t increases with increase in the concentration of the surfactant (NaAOT) in spite of the increase in the viscosity. D_t is higher than the self diffusion coefficient of AOT^- (D_{AOT}). Faster lateral diffusion i.e. higher D_t value with the loading of more and more NaAOT can be explained by the hopping mechanism [76]. At higher NaAOT concentration the concentration of micelle increases hence the collision frequency between the dye molecule at the surface, with other micelles increases consequently the possibility of transition of the solute (dye) molecule from one surface to the other surface increases, hence the D_t value increases.

Solvation dynamics

A wavelength-dependent Stokes shifts in emission spectra of C-153 and C-480 is observed for all the systems. At the red[1] edge of emission spectra, the observed decay consists of a clear rise (growth) followed by usual decay, and at the blue end of emission spectra, a faster decay is observed which is a clear signature of the solvation dynamics. The representative decays of C-153 in **V**, monitoring at three different wavelengths at 298 K are shown in Fig. 4. The red edge and extreme blue edge decay profiles were best fitted by biexponential and triexponential functions, respectively because χ^2 lies close to 1, which indicates the goodness of the fit. The TRES plot of C-153 and C-480 in **V** is shown in Fig. 5.

The $C(t)$ versus time plots are shown in Fig. 6. The decay parameters of $C(t)$ are summarized in Table 4. In our case the average

[1] For interpretation of color in Fig. 4, the reader is referred to the web version of this article.

Table 4
Decay parameters of $C(t)$ of C-153 and C-480 (excluding the missing component) in different systems.

System	a_1	τ_1 (ns)	a_2	τ_2 (ns)	a_3	τ_3 (ns)	$<\tau_s>$[a] (ns)
C-153 in **I**	0.05	0.11	0.04	0.86			0.04
C-153 in **II**	0.17	0.24	0.02	1.78			0.08
C-153 in **III**	0.16	0.37	0.04	2.80	0.01	0.05	0.17
C-153 in **IV**	0.39	0.69	0.12	11.94	0.14	0.11	1.72
C-153 in **V**	0.39	0.77	0.14	13.42	0.06	0.14	2.19
C-153 in **VI**	0.10	0.30	0.16	0.60			0.13
C-153 in $bmimBF_4$[b]	0.47	0.22	0.18	1.34			0.34
C-480 in **I**	0.08	0.15	0.04	0.76			0.04
C-480 in **II**	0.09	0.37	0.04	1.14			0.08
C-480 in **III**	0.12	0.41	0.04	3.01			0.17
C-480 in **IV**	0.26	0.56	0.06	5.81			0.49
C-480 in **V**	0.29	0.69	0.10	9.01			1.10
C-480 in **VI**	0.04	0.27	0.02	0.56			0.02
C-480 in $bmimBF_4$[c]	0.10	0.19	0.19	0.82			0.17

[a] Experimental error of ±0.09 ns, $\tau_i < 100$ ps is missing owing to our instrumental resolution.
[b] These data's in neat ionic liquid ($bmimBF_4$) is taken from Ref. [80].
[c] These data's in neat ionic liquid ($bmimBF_4$) is taken from Ref. [81].

solvation time of C-153 at 298 K in aqueous solution of 4 mM NaAOT was found to be 0.13 ns with components 0.30 ns (10%) and 0.60 ns (16%). In neat ionic liquid ($bmimBF_4$) the average solvation time of C-153 at 298 K is 0.34 ns with components 1.34 ns (18%) and 0.22 ns (47%) and with the addition of water i.e. in water–$bmimBF_4$ the average solvation time changes to 0.04 ns with components 0.86 ns (4%) and 0.11 ns (5%). In case of C-480 the average solvation time in neat ionic liquid ($bmimBF_4$) at 298 K is 0.17 ns with components 0.82 ns (19%) and 0.19 ns (10%) and with the addition of water i.e. in water–$bmimBF_4$ the average solvation time changes to 0.04 ns with components 0.76 ns (4%) and 0.15 ns (8%). We can explain this by considering the structural changes occurred within the ionic liquid with the addition of water. In neat ionic liquid there is significant cation–cation aggregation [79] (head to head), and the ion pairing is mediated by C—H···F hydrogen bonds i.e. the hydrogen bond between imidazolium ring hydrogen and the fluorine of the BF_4^- anion. Added water binds both to the anion and cation. The imidazolium–imidazolium interactions are loosened by the presence of water, which acts as hydrogen bond competitor: C—H···F interactions are progressively replaced by C—H···O (H_2O) hydrogen bonds.

With the loading of NaAOT above CMC the average solvation time increases from 0.17 ns to 2.19 ns in case of C-153 whereas in case of C-480 the average solvation time increases from 0.17 ns to 1.10 ns. This can be explained by the fact that with increase in surfactant concentration the RTIL ($bmimBF_4$) which is free become bound to the micelle (vide supra). From Table 4 it is clear that in case of C-153 the fast component of solvation changes from 0.37 ns (16%) to 0.77 ns (39%), whereas the slow component changes from 2.80 ns (4%) to 13.42 ns (14%) on going from **III** to **V**. This huge change in the slow component (4.79 times) can be explained by the fact that a large fraction of the $bmim^+$ cation is bound to the AOT^- and the binding is cooperative [30]. The anion of the ionic liquid (BF_4^-) also binds with the micelle but the extent of binding is less compared to that of the cation ($bmim^+$) [32] hence the fast component changes only by a factor of 2.08. On the other hand in case of C-480 the fast component of solvation changes from 0.41 ns (12%) to 0.69 ns (29%), whereas the slow component changes from 3.01 ns (4%) to 9.01 ns (10%) on going from **III** to **V**. So in case of C-480 the slow component changes by a factor of 3.0 and the fast component changes by a factor of 1.7. So this also supports the fact that large fraction of $bmim^+$ cation which are free become bound with the AOT^- with the gradual addition of NaAOT. Not only this, the contribution of the fast component changes from 16% to 39% (2.44 times) and from 12% to 29% (2.42 times) for C-153 and C-480 respectively, whereas the contribution of the slow component changes from 4% to 14% (3.50 times) and 4% to 10% (2.5 times) for C-153 and C-480 respectively, which is also in agreement with the fact that the cation binding is more prominent than the anion binding. Interestingly, if we compare the solvation dynamics in case of C-153 and C-480, we can conclude that solvation dynamics is affected more in case of C-153 than C-480. This probe-dependent solvation dynamics [62] can be explained by considering different location of the probe molecules, which is already proved by steady state studies. C-153 being hydrophobic in nature, resides in the stern layer and the adsorption of the $bmim^+$ at the interface modifies stern layer more effectively. So we have observed more pronounced change in solvation dynamics in case of C-153 compared to that in case of C-480. Another important fact is that one cannot explain the dependence of average solvation time with viscosity of the medium alone. On going from water–$bmimBF_4$ mixture to **V**, the viscosity changes by a factor of 18.80 whereas the average solvation time changes by a factor of 54.75 and 27.50 in case of C-153 and C-480 respectively. In case of C-153 the fast component of solvation slows down by a factor of 2.14 and in case of C-480 it reduces by a factor of 1.68 on going from III to V, whereas the diffusion coefficient for the anion (which includes the effect of viscosity and any type of interaction which causes restriction in the movement of the ion) reduces by a factor of 2.39 [32] which indicates that the fast component is mainly due to the motion of anion. The slow component of solvation slows down by a factor of 4.79 and 3.00 in case of C-153 and C-480 respectively, whereas the diffusion coefficient for cation reduces by a factor of 3.46 [28] this clearly indicates that the slow component of the solvation is mainly due to the motion of cation.

Conclusion

This work demonstrates how the interaction between RTIL ($bmimBF_4$) and surfactant (NaAOT) can change the reorientational dynamics of the solvent around the probe molecules C-153 and C-480, having different locations. The difference in the location of the probe molecules is well supported by the absorption, emission and anisotropy experiments. We have shown that with the increase in the concentration of surfactant (NaAOT) the ionic liquid (particularly the cation $bmim^+$) which is initially free, become bound to the surface of NaAOT and the solvation (which is mainly due to the diffusional motion of cation and anion of the ionic liquid) time increases. We have chosen two probes of different polarities to probe the dynamics of two different sites. We have also shown

that, because the adsorption of the $bmim^+$ at the interface modifies stern layer more effectively, the solvation dynamics around the probe molecule, which is located in the stern layer (C-153), is affected more.

Acknowledgements

N.S. thanks the Council of Scientific and Industrial Research (CSIR), and Government of India for generous research Grants. V.G.R, S.M, and S.G are thankful to CSIR and C.B is thankful to UGC for research fellowship.

Appendix A. Supplementary material

Supplementary data associated with this article can be found, in the online version, at http://dx.doi.org/10.1016/j.saa.2012.10.036.

References

[1] K.R. Seddon, Nat. Mater. 2 (2003) 363–365.
[2] S.A. Forsyth, J.M. Pringle, D.R. MacFarlane, Aust. J. Chem. 57 (2004) 113–119.
[3] R.D. Rodgers, K.R. Seddon, Science 302 (2003) 792–793.
[4] T. Welton, Chem. Rev. 99 (1999) 2071–2084.
[5] R.D. Rogers, G.A. Voth, Acc. Chem. Res. 40 (2007) 1077–1078.
[6] M.M. Anna, V. Gallo, P. Mastrorilli, C.F. Nobile, G. Romanazzi, G.P. Suranna, Chem. Commun. (2002) 434–435.
[7] M.L. Dietz, J.A. Dzielawa, Chem. Commun. (2001) 2124–2125.
[8] L.A. Blanchard, D. Hancu, E.J. Beckman, J.F. Brennecke, Nature 399 (1999) 28–29.
[9] S.G. Kazarian, B.J. Briscoe, T. Welton, Chem. Commun. (2000) 2047–2048.
[10] B.M. Quinn, Z. Ding, R. Moulton, A.J. Bard, Langmuir 18 (2002) 1734–1742.
[11] J.A. Laszlo, D.L. Compton, Biotechnol. Bioeng. 75 (2001) 181–186.
[12] J.L. Anderson, V. Pino, E.C. Hagberg, V.V. Sheares, D.W. Armstrong, Chem. Commun. 19 (2003) 2444–2445.
[13] D.F. Evans, A. Yamauchi, G.J. Wei, V.A. Bloomfield, J. Phys. Chem. 87 (1983) 3537–3541.
[14] R. Atkin, G.G. Warr, J. Am. Chem. Soc. 127 (2005) (1941) 11940–11941.
[15] J. Eastoe, S. Gold, S.E. Rogers, A. Paul, T. Welton, R.K. Heenan, J. Am. Chem. Soc. 127 (2005) 7302–7303.
[16] H.X. Gao, J.C. Li, B.X. Han, W.N. Chen, J.L. Zhang, R. Zhang, Phys. Chem. Chem. Phys. 6 (2004) 2914–2916.
[17] Y.A. Gao, N. Li, L.Q. Zheng, X.Y. Zhao, S.H. Zhang, B.X. Han, Green Chem. 8 (2006) 43–49.
[18] T.L. Greaves, A. Weerawardena, C. Fong, C.J. Drummond, Langmuir 23 (2007) 402–404.
[19] J. Lee, M.J. Panzer, Y. He, T.P. Lodge, C.D. Frisbie, J. Am. Chem. Soc. 129 (2007) 4532–4533.
[20] J.C. Hao, A.X. Song, J.Z. Wang, X. Chen, W.C. Zhuang, F. Shi, Chem. Eur. J. 11 (2005) 3936–3940.
[21] K. Behera, S. Pandey, J. Phys. Chem. B 111 (2007) 13307–13315.
[22] R. Rai, G.A. Baker, K. Behera, P. Mohanty, N.D. Kurur, S. Pandey, Langmuir 26 (2010) 17821–17826.
[23] K. Behera, S. Pandey, Langmuir 24 (2008) 6462–6469.
[24] K. Behera, S. Pandey, J. Colloid Interface Sci. 331 (2009) 196–205.
[25] K. Behera, P. Dahiya, S. Pandey, J. Colloid Interface Sci. 307 (2007) 235–245.
[26] S. Shimizu, W.M. McLaren, N. Matubayasi, J. Chem. Phys. 124 (2006) 234905–234908.
[27] N.A. Smirnova, A.A. Vanin, E.A. Safonova, I.B. Pukinsky, Y.A. Anufrikov, A.L. Makarov, J. Colloid Interface Sci. 336 (2009) 793.
[28] K. Behera, M.D. Pandey, M. Porel, S. Pandey, J. Chem. Phys. 127 (2007) 184501–184510.
[29] L. Zheng, C. Guo, J. Wang, X. Liang, S. Chen, J. Ma, B. Yang, Y. Jiang, H. Liu, J. Phys. Chem. B 111 (2007) 1327–1333.
[30] S. Dey, A. Adhikari, D.K. Das, D.K. Sasmal, K. Bhattacharyya, J. Phys. Chem. B 113 (2009) 959–965.
[31] J. Rogers, P.A. Winsor, Nature 216 (1967) 477–479.
[32] S. Murgia, G. Palazzo, M. Mamusa, S. Lampis, M. Monduzzi, J. Phys. Chem. B 113 (2009) 9216–9225.
[33] M. Maroncelli, G.R. Fleming, J. Chem. Phys. 86 (1987) 6221–6239.
[34] N. Nandi, K. Bhattacharyya, B. Bagchi, Chem. Rev. 100 (2000) 2013–2045.
[35] B. Bagchi, Chem. Rev. 105 (2005) 3197–3219.
[36] K. Bhattacharyya, Acc. Chem. Res. 36 (2003) 95–101.
[37] S. Balasubramanian, S. Pal, B. Bagchi, Phys. Rev. Lett. 89 (2002) 115505–115508.
[38] D. Mandal, S. Sen, K. Bhattacharyya, T. Tahara, Chem. Phys. Lett. 359 (2002) 77–82.
[39] P.F. Barbara, W. Jarzeba, Adv. Photochem. 15 (1990) 1–68.
[40] P.J. Rossky, J.D. Simon, Nature 370 (1994) 263–269.
[41] D. Banerjee, S.K. Pal, J. Phys. Chem. A 112 (2008) 7314–7320.
[42] R.K. Mitra, S.S. Sinha, S.K. Pal, Langmuir 24 (2008) 49–56.
[43] P. Mukherjee, J.A. Crank, M. Halder, D.W. Armstrong, J.W. Petrich, J. Phys. Chem. A 110 (2006) 10725–10730.
[44] R. Adhikary, C.A. Barnes, J.W. Petrich, J. Phys. Chem. B 113 (2009) (2004) 11999–12004.
[45] N. Sarkar, K. Das, A. Datta, S. Das, K. Bhattacharyya, J. Phys. Chem. 100 (1996) 10523–10527.
[46] N.E. Levinger, Curr. Opin. Colloid Interface Sci. 5 (2000) 118–124.
[47] P. Sen, S. Ghosh, K. Sahu, S.K. Mondal, D. Roy, K. Bhattacharyya, J. Chem. Phys. 124 (2006) 204905–204912.
[48] P. Hazra, D. Chakrabarty, N. Sarkar, Chem. Phys. Lett. 371 (2003) 553–562.
[49] M. Kumbhakar, S. Nath, T. Mukherjee, H. Pal, J. Chem. Phys. 121 (2004) 6026–6033.
[50] M. Maroncelli, G.R. Fleming, J. Chem. Phys. 89 (1988) 5044–5069.
[51] J.S. Bader, D. Chandler, Chem. Phys. Lett. 157 (1989) 501–504.
[52] K. Bhattacharyya, Chem. Commun. (2008) 2848–2857.
[53] B. Bagchi, B. Jana, Chem. Soc. Rev. 39 (2010) 1936–1954.
[54] S. Balasubramanian, B. Bagchi, J. Phys. Chem. B 106 (2002) 3668–3672.
[55] S. Pal, S. Balasubramanian, B. Bagchi, J. Phys. Chem. B 107 (2003) 5194–5202.
[56] S. Vajda, R. Jimenez, S.J. Rosenthal, V. Fidler, G.R. Fleming, E.W. Castner Jr., J. Chem, Soc, Faraday Trans. 91 (1994) 867–873.
[57] M.L. Horng, J.A. Gardecki, A. Papazyan, M. Maroncelli, J. Phys. Chem. 99 (1995) 17311–17337.
[58] S. Arzhantsev, H. Jin, G.A. Baker, M. Maroncelli, J. Phys. Chem. B. 111 (2007) 4978–4989.
[59] H. Jin, G.A. Baker, S. Arzhantsev, J. Dong, M. Maroncelli, J. Phys. Chem. B 111 (2007) 7291–7302.
[60] C.F. Chapman, M. Maroncelli, J. Phys. Chem. 95 (1991) 9095–9114.
[61] E. Bart, A. Meltsin, D. Huppert, J. Phys. Chem. 98 (1994) 10819–10823.
[62] R. Karmakar, A. Samanta, J. Phys. Chem. A 106 (2002) 6670–6675.
[63] R. Karmakar, A. Samanta, J. Phys. Chem. A 106 (2002) 4447–4452.
[64] S. Bose, R. Adhikary, P. Mukherjee, X. Song, J.W. Petrich, J. Phys. Chem. B 113 (2009) 11061–11068.
[65] P. Mukherjee, J.A. Crank, P.S. Sharma, A.B. Wijeratne, R. Adhikary, S. Bose, D.W. Armstrong, J.W. Petrich, J. Phys. Chem. B 112 (2008) 3390–3396.
[66] X. Song, J. Chem. Phys. 131 (2009) 044503–044508.
[67] M. Halder, L.S. Headley, P. Mukherjee, X. Song, J.W. Petrich, J. Phys. Chem. A 110 (2006) 8623–8626.
[68] Y. Shim, M.Y. Choi, H.J. Kim, J. Chem. Phys. 122 (2005) 44511–44522.
[69] M.N. Kobrak, V. Znamenskiy, Chem. Phys. Lett. 395 (2004) 127–132.
[70] X.H. Huang, C.J. Margulis, Y.H. Li, B.J. Berne, J. Am. Chem. Soc. 127 (2005) 17842–17851.
[71] H.K. Kashyap, R. Biswas, J. Phys. Chem. B 114 (2010) 254–268.
[72] P. Hazra, D. Chakrabarty, N. Sarkar, Langmuir 18 (2002) 7872–7879.
[73] R.S. Fee, M. Maroncelli, J. Chem. Phys. 183 (1994) 235–247.
[74] L.S. Headley, P. Mukherjee, J.L. Anderson, R. Ding, M. Halder, D.W. Armstrong, X. Song, J.W. Petrich, J. Phys. Chem. A 110 (2006) 9549–9554.
[75] K. Behera, S. Pandey, H. Om, J. Phys. Chem. B 113 (2009) 786–793.
[76] N.C. Maiti, M.M.G. Krishana, P.J. Britto, N. Perasamy, J. Phys. Chem. B 101 (1997) 11051–11060.
[77] K.S. Kinosita, S. Kawato, A. Ikegami, Biophys. J. 20 (1977) 289–305.
[78] G. Lipari, A. Szabo, Biophys. J. 30 (1980) 489–506.
[79] M. Moreno, F. Castiglione, A. Mele, C. Pasqui, G. Raos, J. Phys. Chem. B 112 (2008) 7826–7836.
[80] D. Seth, A. Chakraborty, P. Setua, N. Sarkar, J. Phys. Chem. B 111 (2007) 4781–4787.
[81] R. Pramanik, S. Sarkar, C. Ghatak, P. Setua, N. Sarkar, Phys. Chem. Chem. Phys. 12 (2010) 3878–3886.